Determinants of cytoplasmic microtubule depolymerization during ciliogenesis in *Chlamydomonas reinhardtii*

Larissa L Dougherty[1], Prachee Avasthi[1,,§,*]

[1]Biochemistry and Cell Biology Department, Geisel School of Medicine at Dartmouth College, Hanover, New Hampshire
[§]Address correspondence to prachee.avasthi@dartmouth.edu at Geisel School of Medicine at Dartmouth College
[*]Prachee Avasthi is the CSO at Arcadia Science

Abbreviations

- CytoMT/CytoMTs = Cytoplasmic Microtubules
- IFT = Intraflagellar Transport
- MS = Mechanical Shear
- PTX = Paclitaxel

ABSTRACT

At the core of cilia are microtubules which are important for establishing length and assisting ciliary assembly and disassembly; however, another role for microtubule regulation on ciliogenesis lies outside of the cilium. The microtubule cytoskeleton is a highly dynamic structure which polymerizes and depolymerizes rapidly to assist in cellular processes. These processes have been studied across various organisms with chemical as well as genetic perturbations. However, these have generated conflicting data in terms of the role of cytoplasmic microtubules (CytoMTs) and free tubulin dynamics during ciliogenesis. Here we look at the relationship between ciliogenesis and cytoplasmic microtubule dynamics in *Chlamydomonas reinhardtii* using chemical and mechanical perturbations. We find that not only can stabilized CytoMTs allow for normal ciliary assembly, but high calcium concentrations and low pH-induced deciliation cause CytoMTs to depolymerize separately from ciliary shedding. In addition, we find that ciliary shedding through mechanical shearing, cilia regenerate earlier despite intact CytoMTs. Our data suggests that cytoplasmic microtubules are not a sink for a limiting pool of cytoplasmic tubulin in *Chlamydomonas*, depolymerization that occurs following deciliation is a consequence rather than a requirement for ciliogenesis, and intact CytoMTs in the cytoplasm and the proximal cilium support more efficient ciliary assembly.

INTRODUCTION

Ciliogenesis describes the formation of cilia which are microtubule extensions from the plasma membrane that serve as signaling and sometimes motile components of quiescent cells (Tucker et al., 1979). These largely microtubule-based structures are assembled and maintained through intraflagellar transport (IFT) where tubulin monomers among other components are taken to the tip of the cilium for ciliary assembly and maintenance (Craft et al., 2015; Kozminski et al., 1993). This process is influenced by not only the core proteins required for IFT, but also ciliary gene transcription, protein synthesis, trafficking, and complex pre-assembly occurring outside of the cilium. All of the required structures and components generate a highly regulated structure and signaling environment within cilia, and because of this, disruptions to any of these components can lead to various diseases (Reiter & Leroux, 2017). Therefore, it is important to understand how manipulation of cellular processes and components can influence ciliary assembly.

While cilia are themselves a microtubule superstructure, microtubules are also highly dynamic components elsewhere in the cell. They provide structure and polarity to the cell, serve as highways for molecular trafficking, and facilitate cell division among many other roles (de Forges et al., 2012; Parker et al., 2014). To serve these many roles, tubulin assembles and disassembles very rapidly through the process of dynamic instability which describes how tubulin can disassemble into monomers very quickly from GTP hydrolysis (Alushin et al., 2014; Mitchison & Kirschner, 1984).

Disruption of cytoplasmic microtubule (CytoMT) dynamics has previously been shown to directly impact the ability for cilia to assemble through chemical perturbations. For example, through the use of microtubule inhibitors such as colchicine or colcemid which promote CytoMT depolymerization, cilia cannot assemble at all in Chinese hamster fibroblasts (Stubblefield & Brinkley, 1966) *Chlamydomonas* (Rosenbaum et al., 1969) and *Tetrahymena* (Rosenbaum & Carlson, 1969). Conversely, use of the microtubule stabilizer, taxol, has more recently been shown to inhibit acute ciliary elongation in *Chlamydomonas reinhardtii* (Wang et al., 2013). However, while microtubule destabilizing drugs were found to inhibit ciliary assembly, taxol was previously not found to have any effects in PtK1 cells on either assembly or disassembly of primary cilia (Jensen et al., 1987). In contrast, taxol can prevent actin stabilization and microtubule depolymerization-induced ciliary elongation through forskolin, jasplakinolide, and the PKA inhibitor CD. Consistently, the MT depolymerizing drug nocodazole was shown to increase ciliary length likely by freeing up tubulin for ciliogenesis in RPE cells whereas taxol itself shortened cilia (Sharma et al., 2011). Given these cell-type specific and chemical specific discrepancies describing the interplay between CytoMT dynamics and ciliary dynamics, it is important to continue investigating how these processes impact one another to better understand how ciliary dynamics are regulated.

CytoMT dynamics with respect to ciliary dynamics have predominantly been studied through chemical perturbations. Here we explore the requirement for microtubule dynamics in the ciliary model organism *Chlamydomonas reinhardtii* with both chemical perturbations and mechanical perturbations to better understand how microtubule

139 dynamics can regulate ciliary assembly. We ultimately find that total CytoMT
140 depolymerization is not required for ciliary assembly.
141
142 **RESULTS**
143
144 **Paclitaxel-stabilized CytoMTs do not inhibit ciliary assembly to full length in 2**
145 **hours**
146
147 Paclitaxel (PTX), the non-branded Taxol, is a chemical that is well-known for its
148 ability to stabilize microtubules through binding to β-tubulin polymers (Manfredi et al.,
149 n.d.; Parness & Horwitz, 1981). Stabilizing microtubules with taxol has previously been
150 found to shorten steady state length in *Chlamydomonas reinhardtii.* Additionally, it has
151 been found that through common methods of deciliation in *Chlamydomonas*,
152 cytoplasmic microtubules depolymerize. This data led to the hypothesis that tubulin
153 utilized in axonemal assembly for ciliogenesis comes from tubulin present in the cell
154 body (cytoplasmic microtubules, CytoMTs), and microtubule dynamics are required for
155 axonemal microtubule assembly for ciliogenesis (Wang et al., 2013). However, in our
156 previous work, we found that a lower paclitaxel (PTX) concentration from what has
157 previously been utilized for ciliary studies can allow for normal ciliary elongation
158 following pH shock in *Chlamydomonas* which raised the question of whether CytoMT
159 dynamics are truly required for ciliary assembly (Dougherty et al., 2023).
160 We wanted to assess how different PTX concentrations can influence
161 ciliogenesis. To test if taxol is indeed stabilizing CytoMTs at lower concentrations in
162 *Chlamydomonas reinhardtii*, we isolated the soluble ("S") and insoluble ("P") β-tubulin
163 fractions after treating cells with 0.5 M acetic acid to induce deciliation ("pH shock")
164 (Witman et al., 1972), 2 mg/mL colchicine, 1% DMSO, 15 μM PTX, or 40 μM PTX
165 (**Figure 1A**). Following PTX treatment, both 15 μM and 40 μM PTX decreased the
166 presence of β-tubulin in the soluble fraction without completely depleting the pool,
167 confirming that both concentrations sufficiently stabilize CytoMTs in the cells (**Figure 1A**
168 **and 1B**). To directly compare the effect of PTX on ciliogenesis extending beyond
169 steady-state length, cells were treated with increasing concentrations of PTX in the
170 presence or absence of 25 mM lithium chloride (LiCl) (Nakamura et al., 1987).
171 Regardless of PTX concentration, cilia significantly elongated in the presence of LiCl in
172 the CC-1690 wild-type strain in M1 liquid media (**Figure 1C**) previously used in (Wang
173 et al., 2013). We also checked the ability for cilia to completely regenerate from 0 μm
174 through pH shock in the presence of 15 μM PTX, 40 μM PTX, or 60 μM PTX compared
175 to control cells in DMSO (**Figure 1D**). Similarly and consistently with our previous work
176 (Dougherty et al., 2023), cilia regenerated normally in 15 μM PTX, though even at 60
177 μM PTX, ciliary length did not significantly differ from DMSO treated cells at 120
178 minutes (**Figure 1D**). To compare the ability for PTX to stabilize CytoMTs during pH
179 shock, we pretreated cells for 10 minutes with PTX and then fixed and stained them for
180 β-tubulin at 5 minutes post pH shock when microtubules are normally depolymerized
181 (**Figure 1E**). We found that, even immediately following deciliation, CytoMTs are
182 stabilized similarly to pre-deciliated cells as defined by cells which have visible filaments
183 extending past half the long axis of the cell (**Figure 1F**). While this population
184 correlation does not give us changes to tubulin lengths or filament numbers, it

185 provides us with a course measure of how the CytoMT polymerization responds
186 to perturbations. Given that 1) there is already a pool of soluble tubulin at steady state
187 without treatment, 2) decreasing this pool by inducing CytoMT stabilization does not
188 impact ciliogenesis, and 3) increasing this pool by depolymerizing CytoMTs through pH
189 shock also does not impact ciliogenesis, our data suggest that tuning available soluble
190 tubulin access through CytoMT manipulation does not critically impact ciliogenesis.
191

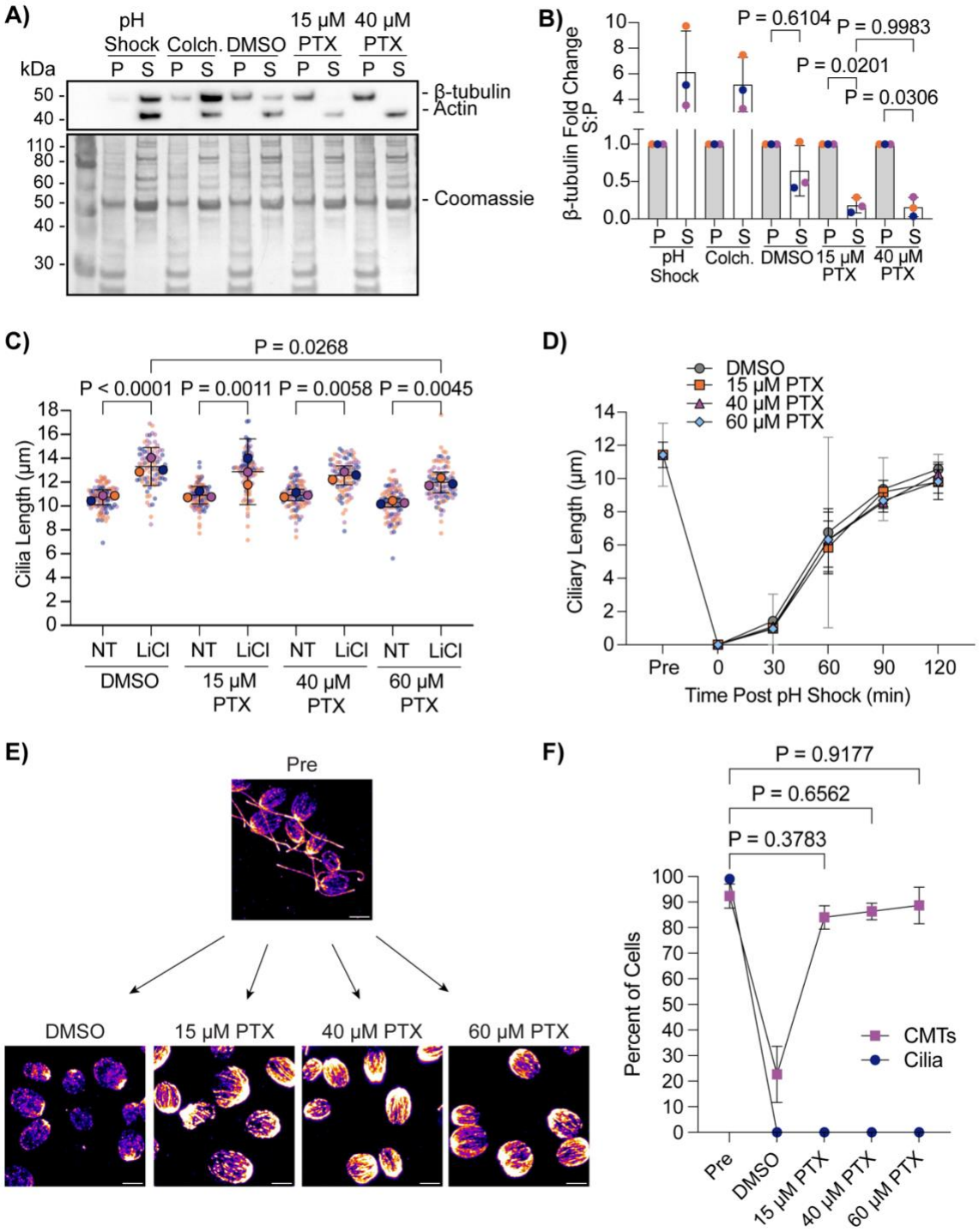

Figure 1. Paclitaxel-stabilized CytoMTs permit normal ciliogenesis. A) Wild-type cells (CC-5325) were treated with acetic acid, 2 mg/mL colchicine for 100 minutes, 1% DMSO for 10 minutes, 15 μM paclitaxel (PTX) for 10 minutes, or 40 μM PTX for 10 minutes. Protein was collected and probed for β-tubulin, actin (soluble protein control), or total protein with Coomassie on a PVDF membrane. **B)** Quantification of western blot band intensity in (**A**). Microtubule intensity was normalized to total protein and then the soluble tubulin (S) intensity was compared to the insoluble intensity (P). Significance was determined using a One-Way

ANOVA with Šídák's multiple comparisons test (N=3). Error bars are mean with standard deviation. For all tests, $P<0.05$ is considered significantly different. **C)** Wild-type cells (CC-1690) were grown in M1 media overnight and then treated with 1% DMSO or increasing concentrations of PTX with or without 25 mM LiCl for 30 min. Significance was determined with a One-Way ANOVA and Šídák's multiple comparisons test (n=30, N=3). **D)** Wild-type cells (CC-5325) were grown in TAP media overnight, pretreated in increasing concentrations of PTX for 10 min, and then regenerated for 2 h after pH shock with acetic acid and PTX. Significance was determined with a One-Way ANOVA and Šídák's multiple comparisons test (n=30, N=2). Error bars are mean with 95% confidence interval. **E)** Representative images of β-tubulin-stained cells at the 5 min timepoint post pH shock in (**D**). Scale bars are 5 µm. **F)** Quantification of the percent of cells with cilia and polymerized cytoplasmic microtubules (CytoMTs) at 5 min post pH shock in DMSO or PTX. Navy blue circles are cilia; purple squares are CytoMTs. Error bars are mean with standard deviation (n=100, N=3). Significance for CytoMTs is represented on the graph and determined using a One Way ANOVA with Šídák's multiple comparisons test. Cells considered to have polymerized microtubules have visible B-tubulin containing filaments extending past half of the cell.

While deciliation and regrowth of cilia from 0 µm is coincident with CytoMT depolymerization and stabilization of CytoMTs does not affect cilium regrowth, we wondered whether cilium growth from cilia maintained at steady state showed similar patterns of CytoMT depolymerization. Acute growth from multiple lengths may indicate whether CytoMTs depolymerization is specific to cilium growth or deciliation. Using 25 mM LiCl to induce ciliary elongation, we checked the polymerization status of CytoMTs across 30 minutes during treatment (**Figure 2A**). Throughout this time, cells were able to elongate ~2 µm as reported in Wang et al., 2013 (**Figure 2B**). However, upon checking CytoMT polymerization throughout this process, we find that these microtubule arrays remained undisturbed in both untreated- and LiCl-treated cells (**Figure 2C**). This data suggests that CytoMT depolymerization is not necessary for ciliary assembly, though it is possible that finer CytoMT depolymerization could occur on a level that is not detectable with these methods.

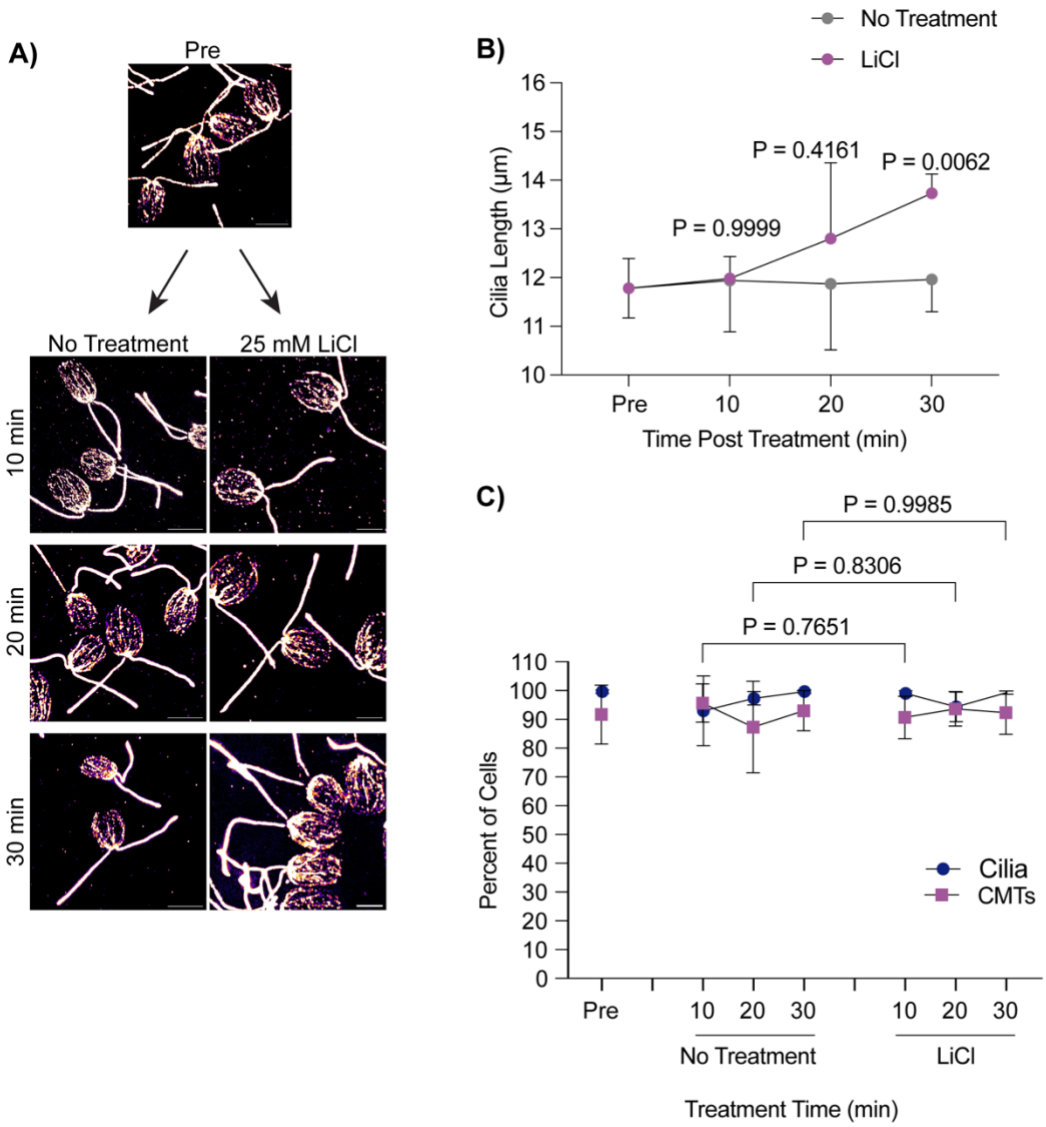

<u>Figure 2. Lithium chloride-induced ciliary elongation does not require CytoMT depolymerization from steady state.</u> A) Wild-type cells were treated with either 25 mM LiCl or no treatment for 30 minutes and then fixed and stained for β-tubulin. Scale bars are 5 µm. **B)** Quantification of cilia length for the experiment described in (**A**). Error bars are mean with 95% confidence interval (n=30, N=3). Significance compares cilia length at 30 min between treatments and was determined with a Two Way ANOVA with Šídák's multiple comparisons test. **C**) Quantification of percent of cells with cilia versus polymerized microtubules for the experiment described in (**A**). Error bars are mean with standard deviation (n=100, N=3). Significance for CytoMTs is represented on the graph and determined using a One-Way ANOVA with Šídák's multiple comparisons test.

Chemically induced ciliary shedding occurs separately from CytoMT depolymerization

Given that CytoMT depolymerization does not occur following ciliary elongation from steady state lengths (**Figure 2**) and cilia assemble to full length in two hours with an available pool of soluble tubulin despite CytoMT stabilization (Figure 1), we suggest that detectable CytoMT depolymerization through pH shock is not a requirement for ciliary assembly. To better understand if depolymerization is a result of physical loss of the cilium versus other factors coincident with cilium loss, we utilized a previously characterized *fa2-1* mutant encoding a mutant NIMA family kinase which cannot deciliate in the presence of calcium or acid (Mahjoub et al., 2002) (**Figure 3A**). Following pH shock, we found that while wild-type cells shed 100% of their cilia and depolymerized ~70% of their CytoMTs (**Figure 3B, left**), the *fa2-1* mutants maintained cilia as expected, but also depolymerized CytoMTs similar to wild-type (**Figure 3B, right**). This is surprising because it was previously reported that CytoMT depolymerization is required for ciliogenesis (Wang et al., 2013), but here we see that even in the absence of deciliation and during pH shock, CytoMTs still depolymerize. This suggests that CytoMT depolymerization could be an artifact or consequence of pH shock and is not strictly tied to loss of cilia.

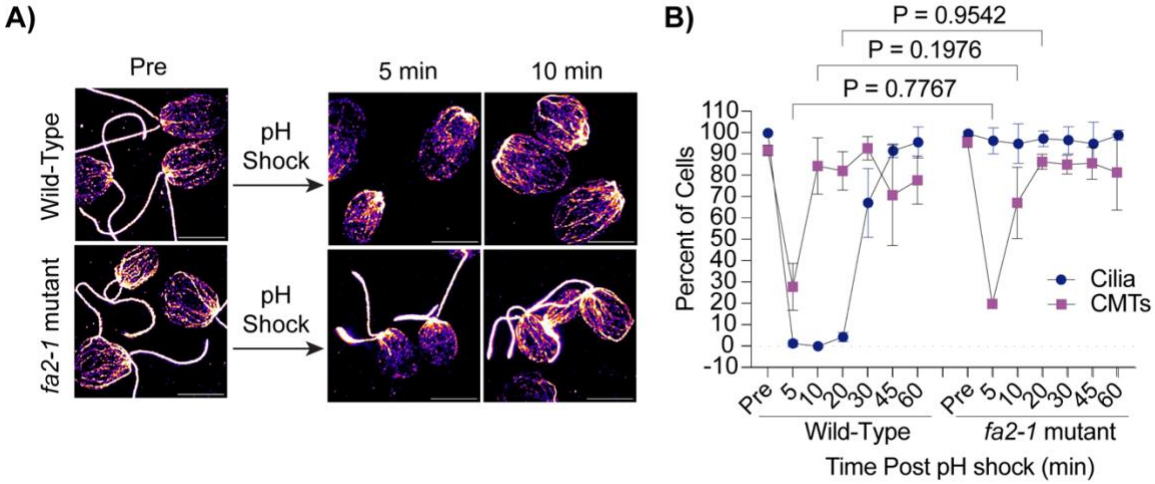

Figure 3. CytoMT depolymerization occurs separately from ciliary shedding following pH shock. A) Wild-type or *fa2-1* mutants were pH shocked with acetic acid for 45 sec and then regrown in fresh TAP for 60 min. Cells were fixed and stained for β-tubulin. Scale bars are 5 µm. **B)** Quantification of percent of cells with cilia or CytoMTs post pH shock. Error bars are mean with standard deviation (n=100, N=3). Significance was determined with a One-Way ANOVA and Šídák's multiple comparisons test for comparisons between CytoMTs.

To test if CytoMT depolymerization was specific to pH shock or if other agents that induce ciliary shedding can also induce CytoMT depolymerization separately. It has previously been established that pH shock induces a calcium influx into the cell (L. M. Quarmby, 1996), and introducing the cell to higher concentrations of calcium can induce ciliary shedding (L. Quarmby & Hartzell, 1994). To further test what triggers CytoMT depolymerization coincident with deciliation, we tested if calcium influx, known to occur upon pH shock, was also sufficient to induce CytoMT depolymerization. We introduced cells to 75 mM calcium chloride ("$CaCl_2$") in 5 mM HEPES ("Buffer") for 10 minutes

which is long enough to induce robust ciliary shedding. Following ciliary shedding, cilia regenerated similar to cilia exposed to pH shock (**Figure 4A**). We then measured the effect of calcium-induced ciliary shedding on CytoMT stability. Upon ciliary shedding, we found that CytoMTs also depolymerized quickly and then reformed similar to pH shock (**Figure 4B).** To determine if calcium has the same effect on ciliated cells, we repeated this experiment in *fa2-1* mutants (**Figure 4C-E**). Similar to wild-type cells, *fa2-1* mutants also exhibited depolymerized microtubules though they did not depolymerize to the same degree as wild-type (**Figure 4E**). This data indicates that depolymerization is specific to calcium-mediated mechanisms rather than cilia loss.

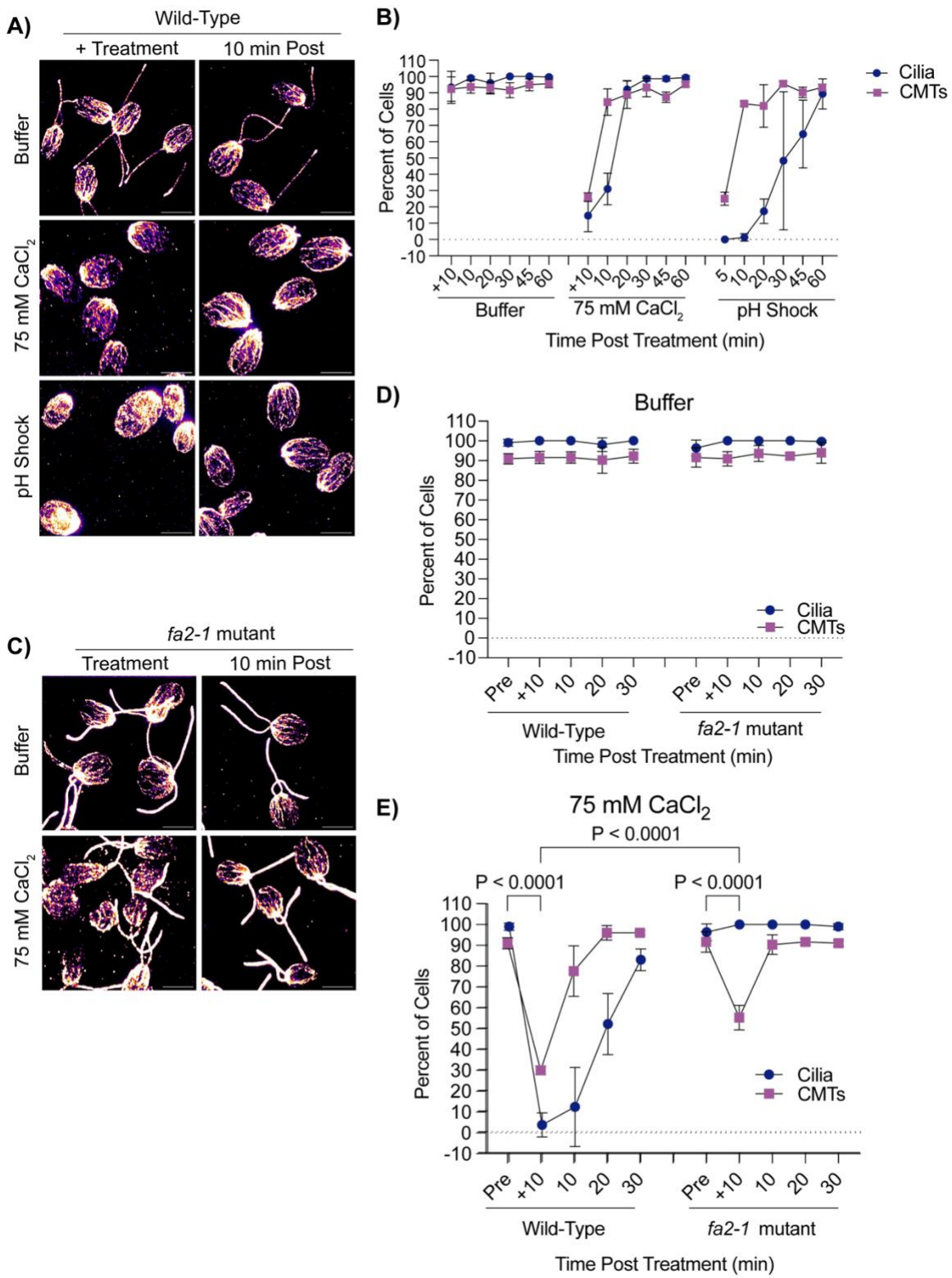

Figure 4. Cytoplasmic microtubule depolymerization occurs separately from ciliary shedding during high calcium. A) Wild-type cells were either pretreated for 10 minutes in 5 mM HEPES ("Buffer"), 10 minutes in 75 mM $CaCl_2$, or 45 seconds in acetic acid, and then fixed and stained for β-tubulin. Scale bars are 5 µm. **B)** Quantification of cilia and

CytoMTs from (**A**). Error bars are mean with standard deviation (n=100, N=3). **C)** Representative images of *fa2-1* mutants following treatment in buffer or 75 mM $CaCl_2$. Cells were fixed and stained for β-tubulin. Scale bars are 5 µm. **D-E**) Quantification of wild-type (CC-5325) or *fa2-1* mutants in buffer (**C**) or 75 mM $CaCl_2$ **(E)**. Error bars are mean with standard deviation (n=100, N=3) for the experiment described in (**C**). Statistics compare CytoMTs and were determined using a One-Way ANOVA and Šídák's multiple comparisons test.

Mechanically sheared cilia do not depolymerize CytoMTs and regenerate cilia faster than following chemical shearing

Next we wanted to assess changes to CytoMT polymerization through non-chemical means of ciliary loss. We introduced the cells to a cell homogenizer/bead beater for 3 minutes to excise cilia and then looked at CytoMTs as cilia regenerated (**Figure 5A**). Interestingly, mechanical shearing did not induce robust CytoMT depolymerization (**Figure 5B**). Further, mechanically sheared cilia were able to regenerate back to full length much faster (in 60 minutes) whereas cilia shed via pH shock were only able to regenerate to half-length in this time (**Figure 5C**). Looking more closely at regeneration in these processes, we found that mechanically sheared cilia, which maintain a ~1 µm ciliary track immediately following ciliary excision, can immediately begin steadily regenerating overtime (**Figure 5C**). In contrast, pH shocked cells have delayed ciliogenesis, but after this process is started, cells can more rapidly regenerate cilia (**Figure 5B-C**). To confirm that this was not a consequence of CytoMT reestablishment, we compared ciliogenesis to CytoMT polymerization. Though pH shocked cells repolymerized CytoMTs within 10-20 minutes, ciliogenesis did not continue until 30-45 minutes post deciliation unlike mechanically sheared cells which maintained both unperturbed CytoMTs and cilia throughout (**Figure 5B-C**). These data show that in the case where cilium growth happens faster, CytoMT depolymerization does not occur. Our data may suggest that polymerized CytoMTs facilitate more rapid ciliogenesis. Alternatively, the existence of cilium initial segments may promote more rapid assembly completely independent of CytoMT state that is dependent instead upon calcium influx (**Figure 4**) that may not be triggered upon mechanical shearing. It could be that initiation of ciliary assembly is rate limiting.

The delay in ciliary shedding due to pH shock may differentially affect CytoMTs based on modifications that add stability. One microtubule modification, acetylation, provides stability, strength, and flexibility to microtubules (Janke & Montagnac, 2017). It's possible that during pH shock, changes to acetylation can occur that may be the cause for the delay in ciliogenesis. To test this, we also compared the presence of acetylated α-tubulin in pH shocked cells versus mechanically sheared cells. Deacetylation of α-tubulin has been found to work in concert with ciliary disassembly during mitosis, and acetylation can act as a signal for downstream events such as cell differentiation in adipocytes (Forcioli-Conti et al., 2016). Acetylation recruits further modifications to tubulin that allow for motility and ciliary length maintenance in *Chlamydomonas* as well as human cells (Tripathi et al., 2021). It is possible that pH shock could be inducing upstream pathways that inhibit CytoMT acetylation must be maintained for ciliogenesis. Comparing pH shock to mechanical shearing, we found that during pH shock, acetylated CytoMTs were significantly shorter both overall (**Figure 5D and E**) and when comparing the longest acetylated CytoMT per cell (**Figure 5D and F**).

These data show that pH shock may affect both stabilized and non-stabilized CytoMTs or affect the degree of acetylation of the stabilized population.

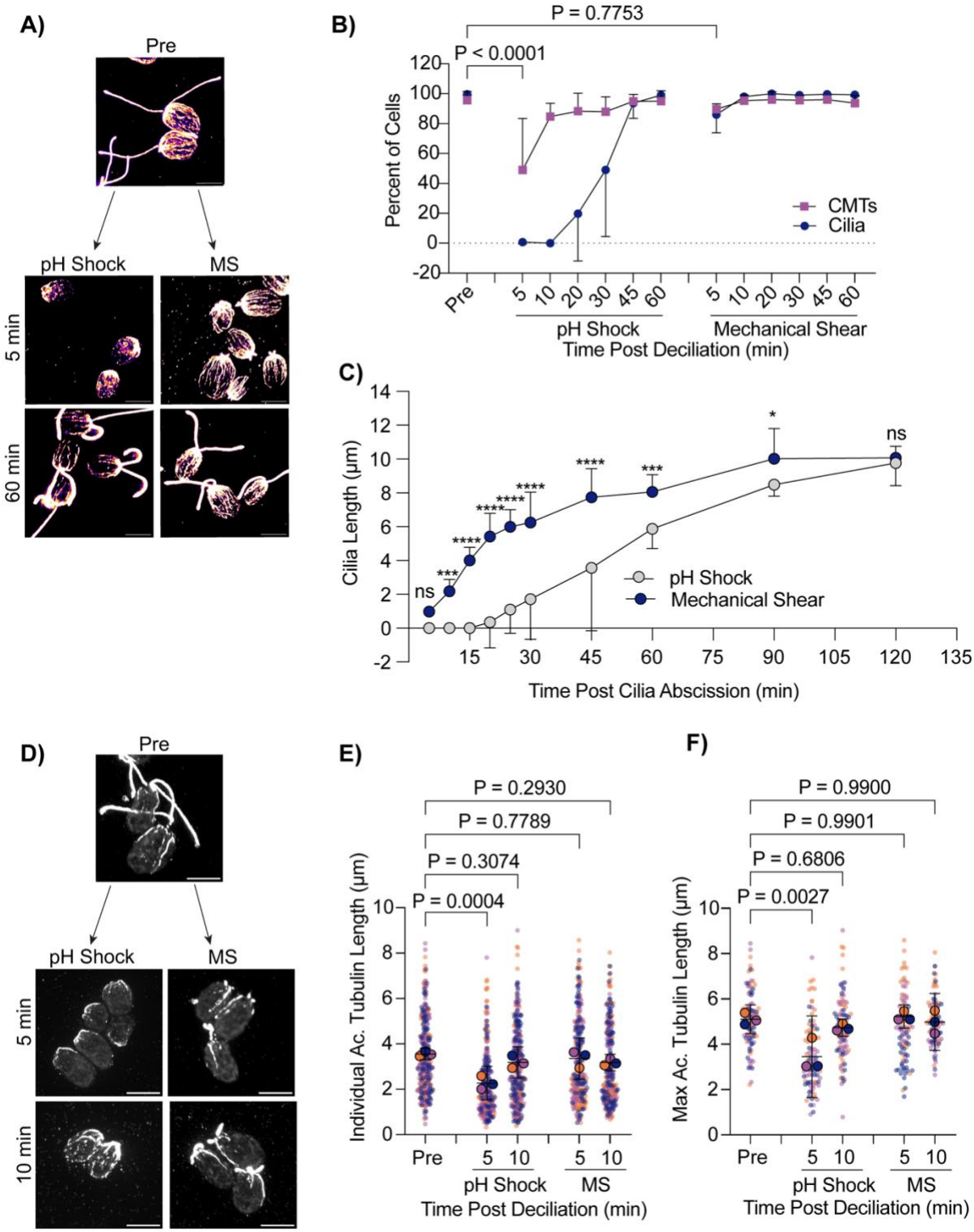

<u>Figure 5. Cells maintain intact cytoplasmic microtubules during mechanical shearing and regenerate cilia more quickly.</u> A) Wild-type cells were either pH shocked for 45 s or placed in a cell homogenizer ("Mechanical Shear", "MS") for 3 minutes. Representative images are cells fixed and stained for β-tubulin. Scale bars are 5 μm. **B)** Quantification of percent of cells with cilia (navy circles) compared to polymerized microtubules (purple squares) between pH shock (left) and MS (right). Error bars are mean with standard deviation. Statistics compare CytoMTs. Significance was determined using a One-Way ANOVA and Šídák's multiple comparisons test (n=30, N=3). **C)** Quantification of cilia length over 2 hours. Error bars are mean with 95% confidence interval (n=30, N=3). Statistics were determined using a Two-Way ANOVA with Šídák's multiple comparisons test (n=30, N=3). (ns - P>0.05, * P≤0.05, ** P≤0.01, *** P≤0.001, **** P≤0.0001). **D)** Wild-type cells were fixed and stained for acetylated α-tubulin following pH shock or MS. Scale bars are 5 μm. **E-F)** Quantification of individual **(E)** or max **(F)** acetylated microtubule lengths. Error bars are mean with 95% confidence interval. Statistics were determined using a One-Way ANOVA and Dunnett's multiple comparisons test (n=30 cells, N=3).

Delayed ciliogenesis upon microtubule depolymerization could indicate that there is a recruitment defect for proteins necessary for ciliogenesis on the cytoplasmic tracks needed for this recruitment or local organization. Using a previously tagged mScarlet-IFT54 anterograde IFT subunit and sfGFP tagged retrograde IFT140 subunit generated and validated by (Wingfield et al., 2021), we compared fluorescence of these complexes at the ciliary base during pH shock and mechanical shear (**Figure S1A and S1C**). We found that during pH shock, there is a significant and more robust increase in fluorescence at the base of cilia for both anterograde (**Figure S1A and S1B**) and retrograde (**Figure S1C and S1D**) trafficking complexes during pH shock as compared to mechanical shearing which remains increased at 10 minutes when CytoMTs have reformed (**Figure 3B)**. The mitigation of the robust increase in mechanically sheared cells may be due to the availability of a ciliary sink as the cilia are more rapidly growing in this case. In other words, these data suggest two potential factors that impact the quantity of IFT proteins at the ciliary base: 1) the availability of CytoMTs for organization or recruitment of IFT proteins and 2) the presence of a fast-growing cilium with an existing ~1 μm track that acts as a sink for IFT proteins.

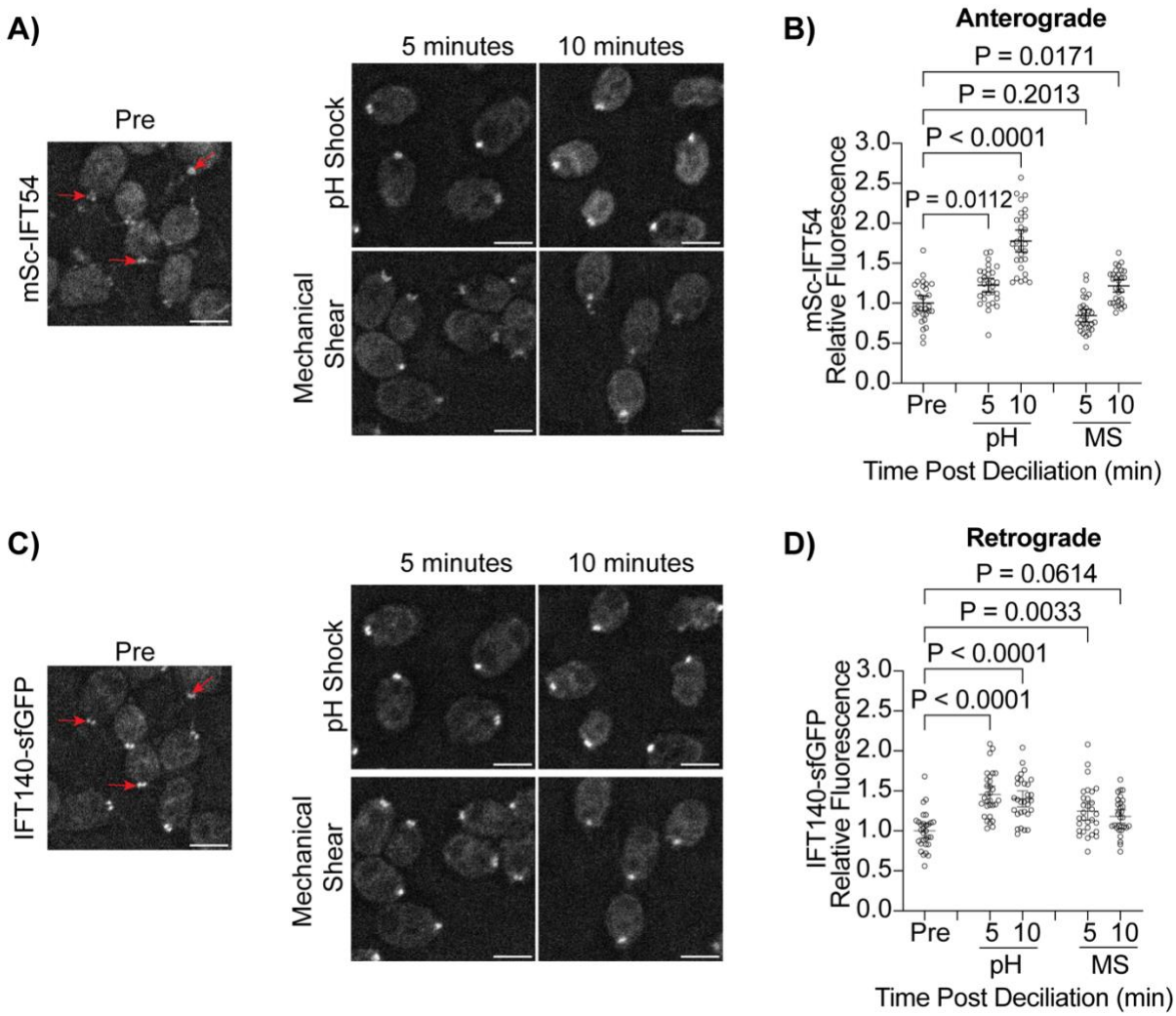

<u>Figure S1. PH shock-induced ciliary shedding increases IFT recruitment to the ciliary base</u>. **A and C)** mSc-IFT54/IFT140-sfGFP were fixed and imaged. Fluorescence at the base of the cilium was quantified (red arrows). Representative images show cells pre deciliation ("Pre"), 5 min, and 10 min post treatment for both pH shock and mechanical shear for both mSc-IFT154 (**A**) and IFT140-GFP (**C**) transport. Scale bars are 5 µm. **B and D)** Quantification of mSc-IFT54 (**B**) or IFT140-sfGFP (**D**) fluorescent intensity at the ciliary base. Error bars are mean with 95% confidence interval (n=30, N=1). Statistics were determined using a One-Way ANOVA and Šídák's multiple comparisons test.

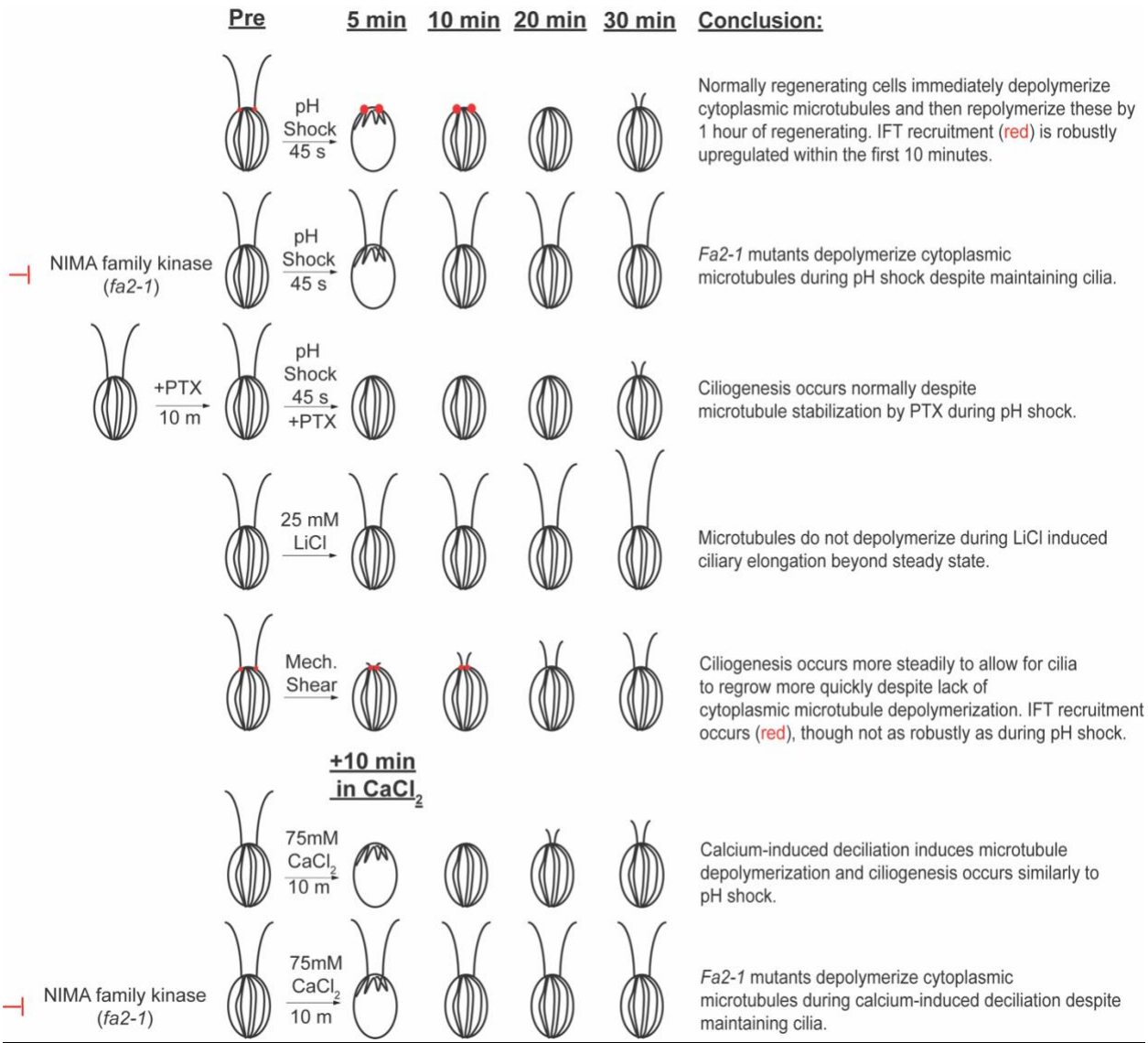

Figure S2. Summary of microtubule dynamics in conjunction with ciliogenesis. Results from each trial are summarized for each of the different conditions tested up to 30 min. Red dots represent IFT fluorescence tested for both pH shock (top) and mechanical shear (bottom). Adapted from (Dougherty et al., 2022).

DISCUSSION

Throughout this work, we identify the relationship between ciliogenesis and CytoMT polymerization which we tease apart by holding either of these processes constant while varying possible determinants. We find that while CytoMT depolymerization does occur during deciliation with some techniques commonly used to induce deciliation, these dynamics are not necessarily required for ciliary assembly and instead may inhibit ciliary assembly due to CytoMT depolymerization as we see a reestablishment in acetylated microtubule length before ciliogenesis can begin (**Figure 5 E-G**) and a need for IFT recruitment to the ciliary base (**Supplemental Figure 1**). These findings are summarized in **Supplemental Figure 2**. Our data are consistent

403 with a model in which events happening during deciliation have effects on associated
404 CytoMT processes, but these are not required for ciliogenesis. These data shed light on
405 two important points: 1) tubulin does not necessarily need to be freed up from the cell in
406 order to allow ciliary assembly to occur; and 2) solubilization of cytoplasmic tubulin is
407 neither required nor does it block the mobilization of the intracellular pool of ciliary
408 protein precursors which we see through stimulated IFT recruitment both during pH
409 shock and mechanical shearing, though this response is less robust during mechanical
410 shearing.
411 While this work addresses the requirement and assembly of tubulin in
412 cytoplasmic microtubules for ciliary dynamics, these experiments are under conditions
413 in which a soluble tubulin pool remains given that there is still a measurable amount of
414 tubulin present both with 15 μM PTX and 40 μM PTX (**Figure 1A and B**). It is possible
415 that this amount of tubulin is enough to supply the start of new cilia while the cell begins
416 generating new tubulin for the assembling cilium which occurs immediately following
417 deciliation (Albee et al., 2013). Soluble tubulin that is not incorporated into tubulin
418 filaments during PTX treatment could be degraded or sequestered, preventing it from
419 bind to other microtubule filaments. It is also possible that the cell homeostasis requires
420 maintenance of some level of soluble tubulin. It has been shown that taxol can induce
421 an increase in tubulin synthesis which makes it likely that the cell can maintain a level of
422 soluble tubulin which can saturate taxol in the cell and give rise to a constant pool of
423 soluble tubulin (Stargell et al., 1992).
424 Effects of pH shock and calcium on live microtubule dynamics alone have
425 previously been investigated (Liu et al., 2017), however the stability of existing
426 microtubules has not been fully explored. Liu et al., 2017 found that, by using mNeon-
427 Green tagged EB1, a microtubule end-binding protein found on the growing end of
428 microtubules, microtubule growth was frozen in *Chlamydomonas* by decreasing pH and
429 increasing calcium concentration. They also noted that the different *Chlamydomonas*
430 tubulin isoforms have different isoelectric points (α-tubulin = 5.01, β-tubulin = 4.82, and
431 EB1 = 5.7), so dropping the pH below these values which allows for sufficient calcium
432 influx to induce ciliary shedding is also sufficient to separately induce CytoMT
433 depolymerization, along with the ability for calcium alone to inhibit microtubule
434 dynamics. However, despite the effect of pH on CytoMT stability shown in this work,
435 there is also a considerable lag between the time that CytoMTs are reestablished and
436 the timing of initial ciliogenesis (**Figure 3B and 5B**) which raises the possibility that
437 other signaling pathways that influence ciliogenesis are inhibited during this process.
438 For example, it was previously found that pH shock activates the microtubule
439 depolymerizing kinesin CrKin13 which has also been implicated in ciliogenesis (Wang et
440 al., 2013).
441 Additionally, this lag in ciliogenesis following pH shock could be due to a lack of
442 CytoMTs altogether for recruitment or organization of proteins needed for ciliary
443 assembly. The well-studied agglutinin protein, SAG1, is one protein which must move
444 from the plasma membrane to the ciliary base upon induction. It has been found that
445 this movement occurs on CytoMTs through the retrograde transport motor cytoplasmic
446 dynein 1b, and following this movement, it can diffuse into the peri-ciliary membrane
447 independent of IFT (Belzile et al., 2014; Cao et al., 2015; Ranjan et al., 2019).
448 Additionally, other ciliary proteins have been found to be assembled in the cytoplasm

before reaching the cilium including the cytoplasmic dynein arm 1I (Viswanadha et al., 2014) and channelrhodopsin which move on acetylated rootlet microtubules through IFT to reach the eyespot (Awasthi et al., 2016; Mittelmeier et al., 2011). During pH shock-induced CytoMT depolymerization, it is possible that without the cytoplasmic highways, proteins cannot reach the ciliary base for transport into the cilium and this is one factor by which ciliogenesis could also be stalled in addition to the delayed build up of IFT at the ciliary base following 10 minutes (**Figure S1B**) when microtubules are repolymerized (**Figure 4A).** Future work needs to be done to better understand how different methods of deciliation can ultimately impact cellular processes that directly regulate ciliogenesis and what molecular factors regulate the entry of proteins already at the base during pH shock-induced deciliation versus other mechanisms of deciliation.

MATERIALS AND METHODS

Strains and Maintenance

The wild-type strains (CC-5325 and CC-1690), *fa2-1* mutant (CC-3751), and IFT strain (ift140-1::IFT140-sfGFP ift54-2::mS-IFT54 mt; CC-5862) were acquired from the *Chlamydomonas* Resource Center. Cells were maintained on 1.5% Tris-Acetate-Phosphate (TAP) plates under constant light. For experiments, CC-1690 cells were inoculated into liquid M1 media, and CC-5325 cells, *fa2-1* mutant cells, and IFT cells were inoculated in TAP and grown overnight under constant light and agitation. All media recipes were used according to the *Chlamydomonas* Resource Center.

Ciliary Length Experiments

Steady State Ciliary Length Experiments: overnight cultures were resuspended in fresh TAP or M1 (CC-1690) the next morning. Cells were treated with either DMSO, paclitaxel (PTX, Invitrogen P3456), Colchicine, or LiCl, fixed in equal amounts of 2% Glutaraldehyde, and then imaged on a Zeiss Axioscope 5 DIC with 40x magnification and Zeiss Zen 3.1 software.

PH Shock-Induced Ciliary Shedding and Regeneration: overnight cultures were resuspended in fresh TAP and pretreated or not with PTX 10 minutes prior to deciliation. To induce deciliation, 0.5 M acetic acid was added to the cell suspension to bring the pH down to 4.5 for 45 sec, and then brought back up to 7.0 with 0.5 M potassium hydroxide. Cells were then spun down at 600xg for 1 minute and resuspended in new TAP with or without PTX.

Calcium Chloride-Induced Ciliary Shedding and Regeneration: overnight cultures resuspended in fresh TAP were spun down for 60 seconds at 600xg at room temperature and resuspended in either 5 mM HEPES or 75 mM calcium chloride in 5 mM HEPES for 10 minutes. Then cells were resuspended in fresh media and allowed to regenerate cilia.

Mechanical Shear-Induced Ciliary Shedding and Regeneration: overnight cultures resuspended in fresh TAP were placed in a cell homogenizer (Analog Disruptor Genie) for 3 minutes, spun down for 60 seconds at 600xg at room temperature, and then resuspended in fresh TAP to regenerate.

495 ***Immunofluorescence and Quantification***
496 **β-Tubulin**: Staining was performed as described in (Wang et al., 2013). Briefly,
497 cells were adhered to poly-lysine coated coverslips, fixed in 30 mM HEPES (pH=7.2), 3
498 mM EGTA, 1 mM $MgSO_4$, and 25 mM KCl with 4% paraformaldehyde ("PFA") for 5
499 minutes, permeabilized with 0.5% NP-40 for 5 minutes, and then fixed in ice cold
500 methanol for 5 minutes. Coverslips were blocked in 5% BSA and 1% Fish ("Block")
501 gelatin for 30 minutes, then in block with 10% Normal Goat Serum ("NGS", Sigma), and
502 then incubated in β-tubulin primary antibody (CST, 2146S) diluted in 20% block in PBS
503 overnight at 4˚C. Coverslips were washed 3x10 minutes in PBS, incubated in secondary
504 antibody (Alexafluor 488 goat anti-rabbit IgG, A11008, 1:500) for 1 hour, washed 3x10
505 minutes in PBS, and allowed to dry. Coverslips were mounted in Fluoromount G
506 (Thermo Scientific) before imaging. Cells were imaged on a Nikon Yokogawa SoRa
507 super resolution spinning disk confocal with 100x oil objective (data collection) and 2.8x
508 magnifier (representative images). For quantification, max immunoprojections were
509 generated from z stacks and 100 cells per time point were counted using the Cell
510 Counter tool in FIJI for either having cytoplasmic microtubules polymerized (spanning >
511 half the cell) or not having microtubules polymerized (spanning < half the cell).
512 **Acetylated α-Tubulin**: Cells adhered to coverslips were fixed in 4% PFA in 10
513 mM HEPES for 15 minutes, placed in ice cold 80% acetone for 5 minutes, placed in ice
514 cold 100% acetone for 5 minutes, and then allowed to dry before rehydrating for 5
515 minutes in PBS. Then cells were blocked in 100% Block for 30 minutes, 10% NGS, and
516 stained for acetylated tubulin (1:1000) overnight at 4˚C. Coverslips were washed 3x10
517 minutes in PBS incubated with secondary (Alexa Fluor 499 goat anti-mouse IgG,
518 Invitrogen A11001) for 1h at RT, covered, and then washed 3x10 minutes in PBS,
519 covered before allowing to dry completely and mount with Fluoromount G. For
520 quantification, max IPs were generated and acetylated microtubules were measured
521 using FIJI's segmented line tool starting at the apex of the cell where acetylated
522 microtubules originate and following along the length of the continuous acetylation
523 signal for 30 cells per timepoint.
524 **IFT140/54**: Cells adhered to coverslips were placed in ice cold 100% methanol
525 2x5 minutes, 50% methanol in PBS for 5 minutes, then PBS for 5 minutes before
526 allowing to dry, mount, and image. For quantification, z stacks were summed together,
527 background subtracted with rolling ball radius = 50, and then equal sized circles drawn
528 over the signal at the base of the cilium. Fluorescent intensity was calculated using the
529 calculation for CTCF as previously described (Dougherty et al., 2023)
530
531 ***SDS-PAGE and Immunoblotting***
532 Soluble (S) and insoluble (P) fractions were collected similarly to (Wang et al.,
533 2013). Briefly, 1 mL of treated cells were collected by centrifugation at 600xg for 1
534 minute at room temperature (RT) and resuspended in 50 µL TMMET Buffer (20 mM
535 Tris-HCl [pH 6.8], 0.14 M NaCl, 1 mM MgCl2, 2 mM EGTA, 4 µg/mL Taxol, and 0.5%
536 Nonidet P-40 Substitute) with 2x30 seconds of vigorous pipetting and 2x30 seconds of
537 gentle vortexing (half-max vortex speed). Cells sat for 10 minutes with 1 gentle round of
538 vortexing at 5 minutes and at 10 minutes before spinning down at 21000xg for 10
539 minutes at room temperature (RT). The supernatant was collected ("S" fraction) and
540 then the pellet was washed with TMMET buffer. Finally, the remaining pellet was

541 resuspended in 100 µL TMMET buffer ("P" fraction). For loading protein samples into
542 the gel, the S fractions were diluted 1:14 in TMMET buffer and P fractions were diluted
543 1:56 in TMMET buffer (determined according to detectable signal within the linear range
544 of the antibodies following blot imaging). Protein from S and P fractions were mixed with
545 2 µL 0.5 M DTT and 4x LDS (Invitrogen), incubated at 70˚C for 10 minutes and run on
546 NuPAGE 10% Bis-Tris gels in MES/SDS-PAGE running buffer (1M MES, 1M Tris base,
547 69.3 mM SDS, 20.5 mM EDTA free acid). Protein was transferred onto PVDF
548 membrane, blocked in 5% milk (w/v, Signature Select Instant Nonfat Dry Milk) in PBST
549 (1x PBS, 0.1% Tween20), incubated in β-tubulin (1:1000, CST 2146S) or actin C4
550 (1:1000, Sigma MAB1501) diluted in 1% milk with 1% BSA in PBST overnight at 4˚C.
551 Blots were washed 3x10 minutes in PBST, incubated in secondary antibody diluted in
552 1% milk with 1% BSA (1:5000, Invitrogen G21234; 1:5000, Invitrogen, 31430) for 1 hour
553 at RT. Blots were washed 3x10 minutes in PBST and then incubated with Pico
554 Chemiluminescent substrate (Invitrogen) and imaged on the Syngene GBOX CHEMI
555 XR 5 using GeneSys software.
556
557 ***Statistical Analysis***
558 Data was collected and organized in Excel, and then graphed and analyzed with
559 GraphPad Prism Version 9.5.1 (528). SuperPlots were made and analyzed according to
560 (Lord et al., 2020) where statistics were performed on the averages of 3 trials and
561 individual trials are represented by corresponding symbol colors. For experiments, "n" is
562 the number of cells quantified and "N" is the number of experiments.
563
564 **ACKNOWLEDGEMENTS**
565
566 We would like to thank the Barlowe Lab at Dartmouth College and Brae Bigge at
567 Arcadia Science for their feedback on experimental ideas and revising the manuscript.
568 We would like to thank Karl Lechtreck for his close reading of the manuscript and
569 catching an error in mutant identification. We would like to thank reviewers for their
570 constructive suggestions to enhance the clarity of the manuscript. We would also like to
571 thank Ann Lavanway at the Life Sciences Light Microscopy Facility at Dartmouth for
572 help with microscopy. We would also like to thank the Biochemistry and Cell Biology
573 Department at Dartmouth College for providing resources to complete this work. This
574 work was funded by NIH MIRA R35GM128702(PA).
575
576
577 **REFERENCES**
578
579 Albee, A. J., Kwan, A. L., Lin, H., Granas, D., Stormo, G. D., & Dutcher, S. K. (2013).
580 Identification of cilia genes that affect cell-cycle progression using whole-genome
581 transcriptome analysis in chlamydomonas reinhardtti. *G3: Genes, Genomes,*
582 *Genetics*, *3*(6), 979–991. https://doi.org/10.1534/g3.113.006338

583 Alushin, G. M., Lander, G. C., Kellogg, E. H., Zhang, R., Baker, D., & Nogales, E.
584 (2014). High-Resolution Microtubule Structures Reveal the Structural Transitions
585 in αβ-Tubulin upon GTP Hydrolysis. *Cell*, *157*(5), 1117–1129.
586 https://doi.org/10.1016/j.cell.2014.03.053
587 Awasthi, M., Ranjan, P., Sharma, K., Veetil, S. K., & Kateriya, S. (2016). The trafficking
588 of bacterial type rhodopsins into the Chlamydomonas eyespot and flagella is IFT
589 mediated. *Scientific Reports*, *6*(1), 34646. https://doi.org/10.1038/srep34646
590 Belzile, O., Hernandez-Lara, C., Wang, Q., & Snell, W. J. (2014). Regulated membrane
591 protein entry into flagella is facilitated by cytoplasmic microtubules and does not
592 require IFT. *Bone*, *23*(1), 1–7.
593 https://doi.org/10.1016/j.cub.2013.06.025.Regulated
594 Cao, M., Ning, J., Hernandez-Lara, C. I., Belzile, O., Wang, Q., Dutcher, S. K., Liu, Y., &
595 Snell, W. J. (2015). Uni-directional ciliary membrane protein trafficking by a
596 cytoplasmic retrograde IFT motor and ciliary ectosome shedding. *ELife*, *4*,
597 e05242. https://doi.org/10.7554/eLife.05242
598 Craft, J. M., Harris, J. A., Hyman, S., Kner, P., & Lechtreck, K. F. (2015). Tubulin
599 transport by IFT is upregulated during ciliary growth by a cilium-autonomous
600 mechanism. *Journal of Cell Biology*, *208*(2), 223–237.
601 https://doi.org/10.1083/jcb.201409036
602 de Forges, H., Bouissou, A., & Perez, F. (2012). Interplay between microtubule
603 dynamics and intracellular organization. *The International Journal of*
604 *Biochemistry & Cell Biology*, *44*(2), 266–274.
605 https://doi.org/10.1016/j.biocel.2011.11.009

Dougherty, L. L., Dutta, S., & Avasthi, P. (2022). *ERK pathway activation inhibits ciliogenesis and causes defects in motor behavior, ciliary gating, and cytoskeletal rearrangement* [Preprint]. Cell Biology. https://doi.org/10.1101/2022.05.18.492507

Dougherty, L. L., Dutta, S., & Avasthi, P. (2023). The ERK activator, BCI, inhibits ciliogenesis and causes defects in motor behavior, ciliary gating, and cytoskeletal rearrangement. *Life Science Alliance*, *6*(6), e202301899. https://doi.org/10.26508/lsa.202301899

Forcioli-Conti, N., Estève, D., Bouloumié, A., Dani, C., & Peraldi, P. (2016). The size of the primary cilium and acetylated tubulin are modulated during adipocyte differentiation: Analysis of HDAC6 functions in these processes. *Biochimie*, *124*, 112–123. https://doi.org/10.1016/j.biochi.2015.09.011

Janke, C., & Montagnac, G. (2017). Causes and Consequences of Microtubule Acetylation. *Current Biology*, *27*(23), R1287–R1292. https://doi.org/10.1016/j.cub.2017.10.044

Jensen, C. G., Davison, E. A., Bowser, S. S., & Rieder, C. L. (1987). Primary cilia cycle in PtK1 cells: Effects of colcemid and taxol on cilia formation and resorption. *Cell Motility and the Cytoskeleton*, *7*(3), 187–197. https://doi.org/10.1002/cm.970070302

Kozminski, K. G., Johnson, K. A., Forscher, P., & Rosenbaum, J. L. (1993). A motility in the eukaryotic flagellum unrelated to flagellar beating (Chlamydomonas/ntrelular movement/ultrastcture). *Proc. Natl. Acad. Sci. USA*, *90*(June), 5519–5523.

Liu, Y., Visetsouk, M., Mynlieff, M., Qin, H., Lechtreck, K. F., & Yang, P. (2017). H+- and Na+- elicited rapid changes of the microtubule cytoskeleton in the biflagellated

green alga Chlamydomonas. *ELife*, *6*, e26002. https://doi.org/10.7554/eLife.26002

Lord, S. J., Velle, K. B., Dyche Mullins, R., & Fritz-Laylin, L. K. (2020). SuperPlots: Communicating reproducibility and variability in cell biology. *Journal of Cell Biology*, *219*(6). https://doi.org/10.1083/JCB.202001064

Mahjoub, M. R., Montpetit, B., Zhao, L., Finst, R. J., Goh, B., Kim, A. C., & Quarmby, L. M. (2002). The *FA2* gene of *Chlamydomonas* encodes a NIMA family kinase with roles in cell cycle progression and microtubule severing during deflagellation. *Journal of Cell Science*, *115*(8), 1759–1768. https://doi.org/10.1242/jcs.115.8.1759

Manfredi, J. J., Parness, J., & Horwitz, S. B. (n.d.). *Taxoi Binds to Cellular Microtubules*.

Mitchison, T., & Kirschner, M. (1984). Dynamic instability of microtubule growth. *Nature*, *312*(5991), 237–242. https://doi.org/10.1038/312237a0

Mittelmeier, T. M., Boyd, J. S., Lamb, M. R., & Dieckmann, C. L. (2011). Asymmetric properties of the Chlamydomonas reinhardtii cytoskeleton direct rhodopsin photoreceptor localization. *Journal of Cell Biology*, *193*(4), 741–753. https://doi.org/10.1083/jcb.201009131

Nakamura, S., Takino, H., & Kojima, M. K. (1987). Effect of lithium on flagellar length in Chlamydomonas reinhardtii. *Cell Structure and Function*, *12*(4), 369–374. https://doi.org/10.1247/csf.12.369

Parker, A. L., Kavallaris, M., & McCarroll, J. A. (2014). Microtubules and Their Role in Cellular Stress in Cancer. *Frontiers in Oncology*, *4*. https://doi.org/10.3389/fonc.2014.00153

652 Parness, J., & Horwitz, S. (1981). Taxol binds to polymerized tubulin in vitro. *Journal of*
653 *Cell Biology*, *91*(2), 479–487. https://doi.org/10.1083/jcb.91.2.479
654 Quarmby, L., & Hartzell, H. (1994). Two distinct, calcium-mediated, signal transduction
655 pathways can trigger deflagellation in Chlamydomonas reinhardtii. *Journal of Cell*
656 *Biology*, *124*(5), 807–815. https://doi.org/10.1083/jcb.124.5.807
657 Quarmby, L. M. (1996). Ca2+ influx activated by low pH in Chlamydomonas. *Journal of*
658 *General Physiology*, *108*(4), 351–361. https://doi.org/10.1085/jgp.108.4.351
659 Ranjan, P., Awasthi, M., & Snell, W. J. (2019). Transient Internalization and Microtubule-
660 Dependent Trafficking of a Ciliary Signaling Receptor from the Plasma
661 Membrane to the Cilium. *Current Biology*, *29*(17), 2942-2947.e2.
662 https://doi.org/10.1016/j.cub.2019.07.022
663 Reiter, J. F., & Leroux, M. R. (2017). Genes and molecular pathways underpinning
664 ciliopathies. *Nature Reviews Molecular Cell Biology*, *18*(9), 533–547.
665 https://doi.org/10.1038/nrm.2017.60
666 Rosenbaum, J. L., & Carlson, K. (1969). Cilia regeneration in Tetrahymena and its
667 inhibition by colchicine. *The Journal of Cell Biology*, *40*(2), 415–425.
668 https://doi.org/10.1083/jcb.40.2.415
669 Rosenbaum, J. L., Moulder, J. E., & Ringo, D. L. (1969). Flagellar elongation and
670 shortening in Chlamydomonas: The Use of Cycloheximide and Colchicine to
671 Study the Synthesis and Assembly of Flagellar Proteins. *Journal of Cell Biology*,
672 *41*(2), 600–619. https://doi.org/10.1083/jcb.41.2.600

673 Sharma, N., Kosan, Z. A., Stallworth, J. E., Berbari, N. F., & Yoder, B. K. (2011). Soluble
674 levels of cytosolic tubulin regulate ciliary length control. *Molecular Biology of the*
675 *Cell*, *22*(6), 806–816. https://doi.org/10.1091/mbc.e10-03-0269
676 Stargell, L. A., Heruth, D. P., Gaertig, J., & Gorovsky, M. A. (1992). Drugs affecting
677 microtubule dynamics increase alpha-tubulin mRNA accumulation via
678 transcription in Tetrahymena thermophila. *Molecular and Cellular Biology*, *12*(4),
679 1443–1450. https://doi.org/10.1128/mcb.12.4.1443-1450.1992
680 Stubblefield, E., & Brinkley, B. R. (1966). CILIA FORMATION IN CHINESE HAMSTER
681 FIBROBLASTS IN VITRO AS A RESPONSE TO COLCEMID TREATMENT.
682 *Journal of Cell Biology*, *30*(3), 645–652. https://doi.org/10.1083/jcb.30.3.645
683 Tripathi, P., Zhu, Z., Qin, H., Elsherbini, A., Crivelli, S. M., Roush, E., Wang, G.,
684 Spassieva, S. D., & Bieberich, E. (2021). Palmitoylation of acetylated tubulin and
685 association with ceramide-rich platforms is critical for ciliogenesis. *Journal of*
686 *Lipid Research*, *62*, 100021. https://doi.org/10.1194/jlr.RA120001190
687 Tucker, R. W., Pardee, A. B., & Fujiwara, K. (1979). Centriole ciliation is related to
688 quiescence and DNA synthesis in 3T3 cells. *Cell*, *17*(3), 527–535.
689 https://doi.org/10.1016/0092-8674(79)90261-7
690 Viswanadha, R., Hunter, E. L., Yamamoto, R., Wirschell, M., Alford, L. M., Dutcher, S.
691 K., & Sale, W. S. (2014). The ciliary inner dynein arm, I1 dynein, is assembled in
692 the cytoplasm and transported by IFT before axonemal docking: Assembly of
693 Ciliary Inner Dynein Arms. *Cytoskeleton*, *71*(10), 573–586.
694 https://doi.org/10.1002/cm.21192

Wang, L., Piao, T., Cao, M., Qin, T., Huang, L., Deng, H., Mao, T., & Pan, J. (2013). Flagellar regeneration requires cytoplasmic microtubule depolymerization and kinesin-13. *Journal of Cell Science*, *126*(6), 1531–1540. https://doi.org/10.1242/jcs.124255

Wingfield, J. L., Mekonnen, B., Mengoni, I., Liu, P., Jordan, M., Diener, D., Pigino, G., & Lechtreck, K. (2021). *In vivo* imaging shows continued association of several IFT-A, IFT-B and dynein complexes while IFT trains U-turn at the tip. *Journal of Cell Science*, *134*(18), jcs259010. https://doi.org/10.1242/jcs.259010

Witman, G. B., Carlson, K., Berliner, J., & Rosenbaum, L. (1972). I. Isolation and Electrophoretic Analysis of Microtubules, Matrix, Membranes, and Mastigonemes. *The Journal of Cell Biology*, *54*, 507–539. https://doi.org/10.1083/jcb.54.3.507